Supplemental Data

Kinetochores Use a Novel Mechanism for Coordinating the Dynamics of Individual Microtubules

Kristin J. VandenBeldt, Rita M. Barnard, Polla J. Hergert, Xing Meng, Helder Maiato, and Bruce F. McEwen

Supplemental Experimental Procedures

Specimen Preparation for Electron Microscopy

Monolayers of PtK1 cells were grown at 37ºC in Hams F12 medium with 10% FBS on sapphire discs 0.02 mm thick and 3 mm in diameter (Rudolf Brugger, Minusio, Switzerland). Drug-treated cells were exposed to either 1 μM taxol for 5 min or 1 μM nocodazole for 2 min. Metaphase, taxol-treated, and nocodazole-treated PtK1 cells were prepared by high pressure freezing and freeze substitution, as described previously [S1]. Briefly, discs were dipped in 10% Ficoll (MW 70,000; Sigma, St Louis, MO) in medium and then high-pressure frozen with a Baltec HPM 010. Samples were transferred to a Balzers FSU 010 freeze-substitution device and were substituted in 0.5% glutaraldehyde with 0.1% tannic acid in anhydrous acetone at −90ºC. After 24 hr, the specimens were given three 15 min rinses in anhydrous acetone at −90ºC, followed by substitution in 1.0% OsO_4 with 0.1% uranyl acetate. After 24 hr, samples were allowed to warm to room temperature for approximately 6 hr, rinsed three times in anhydrous acetone, and infiltrated and flat embedded in Epon-Araldite [S2]. Anaphase PtK1 cells and metaphase S2 cells were grown on glass coverslips, fixed in PHEM buffer (60 mM PIPES, 25 mM HEPES, 10 mM EGTA, and 2 mM $MgCl_2$ [pH 6.9]), and processed for electron microscopy as described previously [S3].

Serial sections were cut at a thickness of 150–250 nm on a Reichert Ultracut E ultramicrotome. Serial plastic sections were prescanned for kinetochores at a low magnification on a Zeiss 910 EM, and 10 nm colloidal gold particles were affixed to one side of the selected grids to serve as fiducial markers for subsequent image alignment.

Electron Tomography

Dual-axis tomographic tilt series were digitally recorded on either a Tecnai F20 at 200 kV with a Gatan 2K × 2K CCD camera at a pixel size of 1.6 nm or on a Zeiss 910 at 100 kV with a Gatan (TVIPS) 1K × 1K CCD camera at a pixel size of 1.6 nm [S4]. The tilt-angle increment was varied according to the cosine of the tilt angle, with an increment at the untilted image of 1.5º–2.0º and a total angular range of ±60º to ±70º [S5].

Processing and Analysis of Tomographic Data

Image alignment and computation of tomographic reconstructions were accomplished with a combination of SPIDER and IMOD software. The conformations of kMT plus ends were manually classified by extracting subvolumes from the tomographic reconstructions that each contained a single kMT plus end. Three investigators independently inspected these subvolumes without knowledge of the kMT origin. The conformations of kMT plus ends were classified as straight if they were: (1) straight and even, (2) straight and uneven, (3) straight and capped, or (4) slightly flared (Figure 1D). The conformation of kMT plus ends were classified as curved if they were: (1) coiled or (2) highly flared so that the sides of the plus-end tips curved far enough to at least make a right angle to the length of the tube (Figure 1E). Classification methods were based on published cryo EM images of in vitro assembled MTs [S6–S9]. Using this system, we were able to classify 92%–96% of the plus ends examined for each experimental category. The unclassified plus ends were generally obscured by material surrounding the termination point in the kinetochore and were not included in calculating the bar graphs.

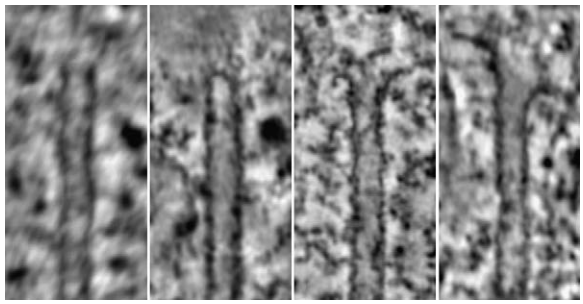

Figure S1. Conformations Observed for the Plus Ends of MTs that Were Not Bound to the Kinetochore or the Spindle Pole

Conformations were similar to those detected for kMT plus ends.

Supplemental References

S1. McEwen, B.F., Hsieh, C.E., Mattheyses, A.L., and Rieder, C.L. (1998). A new look at kinetochore structure in vertebrate somatic cells using high-pressure freezing and freeze substitution. Chromosoma *107*, 366–375.

S2. Rieder, C.L., and Cassels, G. (1999). Correlative light and electron microscopy of mitotic cells in monolayer cultures. Methods Cell Biol. *61*, 297–315.

S3. McEwen, B.F., Heagle, A.B., Cassels, G.O., Buttle, K.F., and Rieder, C.L. (1997). Kinetochore fiber maturation in PtK1 cells and its implications for the mechanisms of chromosome congression and anaphase onset. J. Cell Biol. *137*, 1567–1580.

S4. McEwen, B.F., and Marko, M. (1999). Three-dimensional transmission electron microscopy and its application to mitosis research. Methods Cell Biol. *61*, 81–111.

S5. McEwen, B.F., Marko, M., Hsieh, C.E., and Mannella, C. (2002). Use of frozen-hydrated axonemes to assess imaging parameters and resolution limits in cryoelectron tomography. J. Struct. Biol. *138*, 47–57.

S6. Mandelkow, E.M., Mandelkow, E., and Milligan, R.A. (1991). Microtubule dynamics and microtubule caps: a time-resolved cryo-electron microscopy study. J. Cell Biol. *114*, 977–991.

S7. Chretien, D., Fuller, S.D., and Karsenti, E. (1995). Structure of growing microtubule ends: two-dimensional sheets close into tubes at variable rates. J. Cell Biol. *129*, 1311–1328.

S8. Arnal, I., Karsenti, E., and Hyman, A.A. (2000). Structural transitions at microtubule ends correlate with their dynamic properties in *Xenopus egg* extracts. J. Cell Biol. *149*, 767–774.

S9. Janosi, I.M., Chretien, D., and Flyvbjerg, H. (2002). Structural microtubule cap: stability, catastrophe, rescue, and third state. Biophys. J. *83*, 1317–1330.

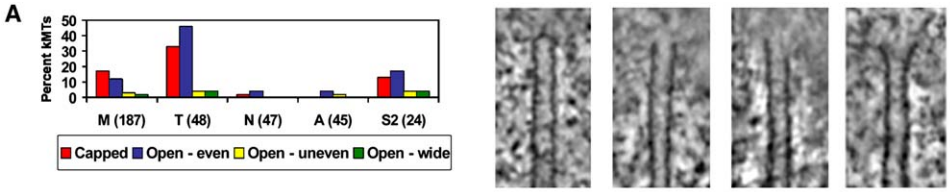

	Total # Straight:	# Capped:	# Open - even:	# Open - uneven:	# Open - wide:
Metaphase (187):	62 (33%)	31 (17%)	23 (12%)	5 (3%)	3 (2%)
Taxol (48):	42 (88%)	16 (33%)	22 (46%)	2 (4%)	2 (4%)
Nocodazole (47):	3 (6%)	1 (2%)	2 (4%)	0 (0%)	0 (0%)
Anaphase (45):	3 (7%)	0 (0%)	2 (4%)	1 (2%)	0 (0%)
S2 (24):	9(38%)	3 (13%)	4 (17%)	1 (4%)	1 (4%)

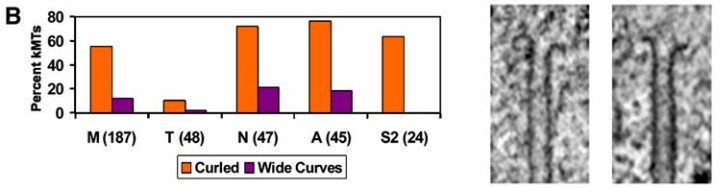

	Total # Curved:	# Curled:	# Wide Curves:
Metaphase (187):	125 (67%)	103 (55%)	22 (12%)
Taxol (48):	6 (13%)	5 (10%)	1 (2%)
Nocodazole (47):	44 (94%)	34 (72%)	10 (21%)
Anaphase (45):	42 (93%)	34 (76%)	8 (18%)
S2 (24):	15 (63%)	15 (63%)	0 (0%)

Figure S2. Summary of Subconformational Classifications

(A) Straight kMT plus ends. The bar graph shows the percentage of total kMT plus ends having conformations similar to each of the images in Figure 1D for: M, untreated metaphase; T, taxol-treated metaphase; N, nocodazole-treated metaphase; A, untreated anaphase PtK_1 cells; and S2, untreated metaphase *Drosophila* S2 cells. The table shows images from Figure 1D above columns that list the number and percentage of the kMT plus ends having a similar conformation.

(B) Curved kMT plus ends. Same representation as in (A) for the two types of images in Figure 1E.

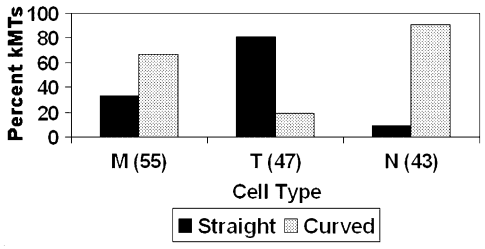

Figure S3. Bar Graph of kMT Plus-End Conformations after Fixation in PHEM Buffer

The percentage of kMT plus ends classified as straight and curved is plotted for: M, untreated metaphase; T, taxol-treated metaphase; and N, nocodazole-treated metaphase PtK_1 cells fixed in PHEM buffer. The sample size is indicated in parentheses on the abscissa. The results are essentially the same as for cells fixed by high-pressure freezing and freeze substitution (Figure 2).

Table S1. Plus-End Conformations of kMTs Terminating in the Corona and Heterochromatin

	Corona (CR)		Heterochromatin (HC)	
	# Straight	# Curved	# Straight	# Curved
Metaphase	0	6	0	10
Taxol	0	0	0	3
Nocodazole	0	1	0	0
Anaphase	0	2	1	1